TẠP CHÍ KHOA HỌC VÀ CÔNG NGHỆ ĐẠI HỌC DUY TÂN
DTU Journal of Science and Technology 05(78) (226) 9-18

ĐẠI HỌC DUY TÂN
DUYTAN UNIVERSITY

Welding Technology for Joining the Bottom Head and Shell of VVER Reactor Pressure Vessels in Vietnam

Công nghệ hàn nối đáy và thân của bình chịu áp lực lò phản ứng VVER tại Việt Nam

Vu Duong[a*], Nguyen Duc Hoang A[b], Dang Nguyen Phuong Uyen[b]
Vũ Dương[a*], Nguyễn Đức Hoàng A[b], Đặng Nguyễn Phương Uyên[b]

[a]*Center of Mechanical Engineering, School of Engineering and Technology, Duy Tan University, Da Nang, 550000, Vietnam*
[a]*Trung tâm Cơ khí, Trường Công nghệ & Kỹ thuật, Đại học Duy Tân, Đà Nẵng, 550000, Việt Nam*
[b]*Faculty of Mechanical Engineering, School of Engineering and Technology, Da Nang, 550000, Vietnam*
[b]*Khoa Cơ khí, Trường Công nghệ & Kỹ thuật, Đại học Duy Tân, Đà Nẵng, 550000, Việt Nam*

(Date of receiving article: 27/01/2026, date of completion of review: 24/07/2026, date of acceptance for posting: 18/09/2026)

Abstract

The circumferential weld joining the bottom head and the cylindrical shell of VVER-class reactor pressure vessels (RPVs) constitutes a structural discontinuity of critical significance. The thermo-mechanical stability of this weld governs vessel service life, irradiation tolerance, and post-weld nondestructive inspectability. This study synthesizes current advances in metallurgy, welding science, microstructural engineering, and AI-enabled process optimization to establish an integrated welding framework for the improved ferritic–bainitic CHSN01 alloy (Fe–Cr–Ni–Mo–Co). The alloy composition is analytically derived, consolidated, and performance-optimized by the authors to meet the functional requirements associated with VVER-grade nuclear pressure-boundary weldments. The proposed welding route incorporates GTAW for the root pass, mechanized narrow-gap SAW for the fill passes, and GMAW/SMAW for the cap layers; dissimilar metal interfaces employ Ni-based buttering to suppress the formation of brittle intermetallic phases. AI-guided Bayesian–genetic optimization is applied to define coupled heat-input and travel-speed domains that minimize distortion while preserving strength and toughness within RPV-class criteria. Drawing on internationally published research from 1980 to 2025, the work provides a coherent technological basis for WPS/PQR qualification and subsequent industrial-scale deployment in Vietnam and Southeast Asia.

Keywords: VVER, reactor pressure vessel, improved CHSN01 alloy, narrow-gap SAW, dissimilar metal welding, post-weld heat treatment (PWHT), AI optimization

Tóm tắt

Mối hàn chu vi nối phần đáy và thân bình chịu áp lực của các bình áp suất lò phản ứng (RPV) loại VVER tạo thành một điểm gián đoạn cấu trúc có ý nghĩa cực kỳ quan trọng. Độ ổn định nhiệt-cơ học của mối hàn này quyết định tuổi thọ của bình, khả năng chịu bức xạ và khả năng kiểm tra không phá hủy sau khi hàn. Nghiên cứu này tổng hợp những tiến bộ hiện tại trong luyện kim, khoa học hàn, kỹ thuật vi cấu trúc và tối ưu hóa quy trình dựa trên trí tuệ nhân tạo để thiết lập một khung hàn tích hợp cho hợp kim CHSN01 ferritic-bainit cải tiến (Fe–Cr–Ni–Mo–Co). Thành phần hợp kim được các tác giả phân tích, củng cố và tối ưu hóa hiệu suất để đáp ứng các yêu cầu chức năng liên quan đến các mối hàn ranh giới áp suất hạt nhân cấp VVER. Quy trình hàn được đề xuất kết hợp hàn GTAW cho lớp hàn gốc, hàn SAW khe hẹp cơ khí cho các lớp hàn lấp đầy và hàn GMAW/SMAW cho các lớp phủ; các giao diện kim loại khác loại sử dụng lớp phủ đệm

[*]*Corresponding author:* Vu Duong
Email: vuduong@duytan.edu.vn

gốc Ni để ngăn chặn sự hình thành các pha liên kim loại giòn. Tối ưu hóa Bayes-Di truyền có hướng dẫn bởi trí tuệ nhân tạo được áp dụng để xác định các miền nhiệt lượng đầu vào và tốc độ di chuyển kết hợp nhằm giảm thiểu biến dạng trong khi vẫn duy trì độ bền và độ dẻo dai theo tiêu chuẩn của bình áp suất lò phản ứng (RPV). Dựa trên các nghiên cứu được công bố quốc tế từ năm 1980 đến năm 2025, công trình này cung cấp cơ sở công nghệ mạch lạc cho việc chứng nhận WPS/PQR và triển khai quy mô công nghiệp tiếp theo tại Việt Nam và Đông Nam Á.

Từ khoá: VVER, bình chịu áp lực lò phản ứng, hợp kim CHSN01 cải tiến, hàn SAW khe hẹp, hàn kim loại khác loại, xử lý nhiệt sau hàn (PWHT), tối ưu hóa AI

1. Introduction

The bottom-head-to-shell weld in VVER reactor pressure vessels is a structural interface subjected to combined internal pressure, neutron irradiation, thermal shock cycles, and long-term embrittlement mechanisms. Its integrity is central to safe long-term operation and regulatory lifetime extension [1, 2]. Microstructural evolution at this location is controlled by welding heat input, post-weld heat treatment (PWHT), alloy chemistry, and irradiation-induced defect dynamics, as documented in contemporary VVER surveillance programs and annealing studies [3, 4].

Modern industrial practice has moved from conventional wide-gap multi-pass welding toward automated narrow-gap welding, solid-state concepts, and hybrid processes [5,6,7]. These transitions have been driven by the need to reduce angular distortion, narrow heat-affected zones, and enhance volumetric inspectability—particularly relevant for thick-section steels in the 180–250 mm class typical of VVER-1000 and VVER-1200 vessels.

Simultaneously, computational metallurgy and machine-learning strategies have begun reshaping alloy design and weld-parameter optimization, enabling predictive correlations of phase transformations, residual-stress relaxation, and irradiation-induced hardening [8]. Large-scale datasets from STRUMAT-LTO and EU RPV ageing projects (2023–2025) have further refined understanding of embrittlement mechanisms and recovery kinetics.

Against this backdrop, the present study aims to synthesize a coherent welding technology framework for Vietnam's emerging nuclear manufacturing capability. The improved CHSN01 alloy, derived from Fe–Cr–Ni–Mo–Co ferritic–bainitic architectures, is taken as the candidate base material for domestically produced VVER vessels. The study follows four objectives:

(1) Define a welding system suitable for thick-section RPV steels**,** integrating GTAW, narrow-gap SAW, and GMAW/SMAW.

(2) Establish filler selection and metallurgical compatibility**,** including Ni-based buttering for dissimilar metal transitions.

(3) Apply AI-based optimization to thermal cycles, heat-input regimes, and residual stress minimization.

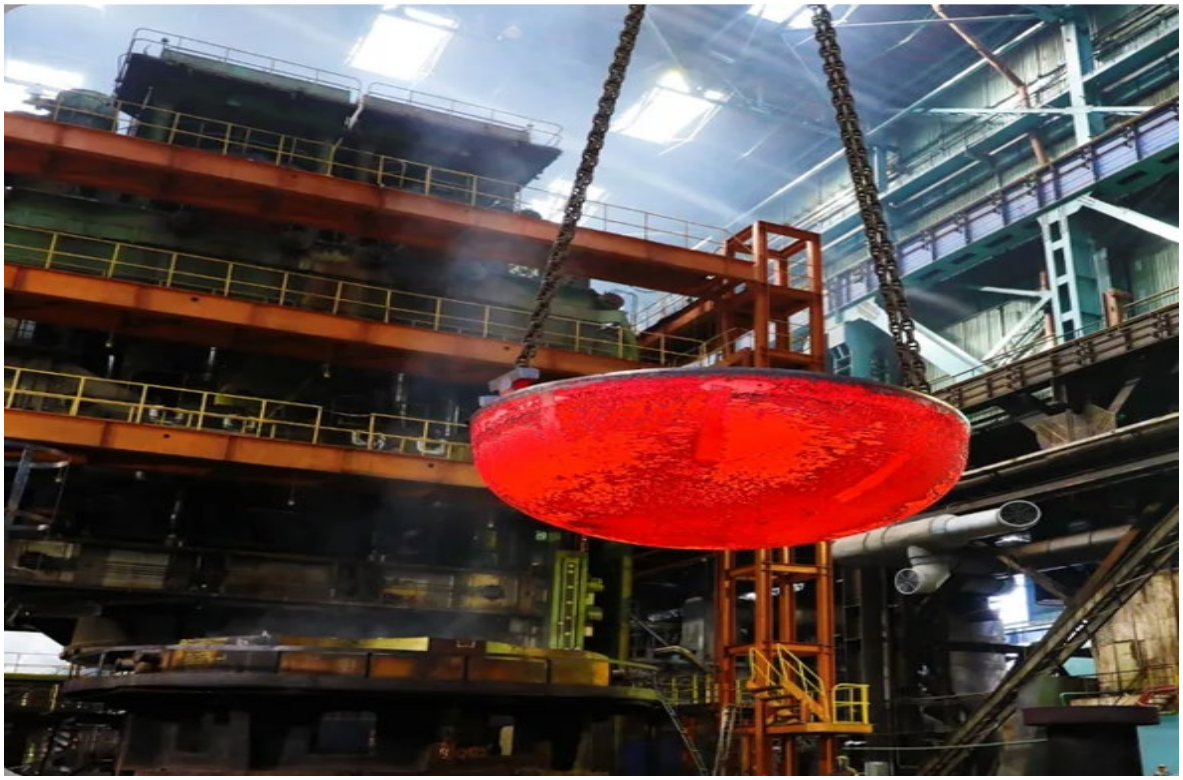


Fig 1. Machining and fabrication of the lower head of a VVER reactor pressure vessel.

Provide a qualification roadmap for WPS/PQR/WPQ and mock-up fabrication for Vietnam and Southeast Asia.

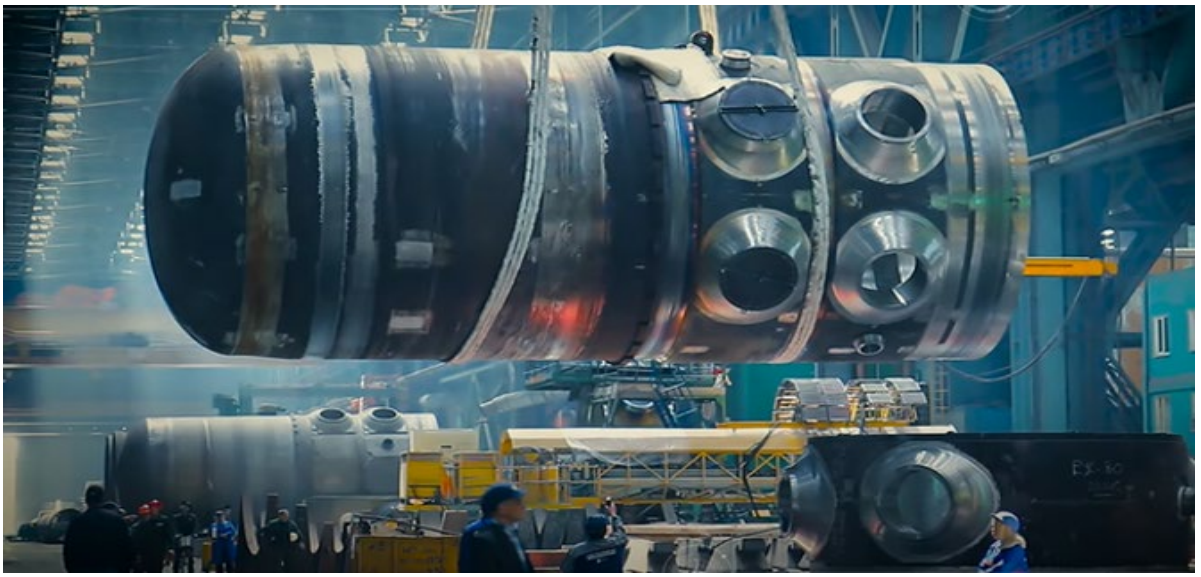


Fig 2. Controlled circumferential welding process for joining the lower head to the cylindrical shell of a VVER reactor pressure vessel.

2. Materials and methods

2.1. Data sources and research scope

This study is grounded in an extensive body of domestic and international research accumulated over several decades, reflecting the continuous evolution of welding technologies—from classical submerged arc welding methods [5, 6] to advanced laser–arc hybrid processes [8]. The principal thematic domains include:

(1) the effects of neutron irradiation on the mechanical properties and microstructural evolution of RPV steels [1, 2];

(2) recovery mechanisms induced by post-irradiation annealing and associated thermo–microstructural transitions [3];

(3) metallurgical compatibility in dissimilar metal welds [9, 10];

(4) modeling and prediction of residual stresses in thick-section components [11].

Table 1 provides a systematic consolidation of the process characteristics of GTAW, GMAW, SAW, EBW, laser–arc hybrid welding, FSW, and WAAM, evaluated within the context of technical requirements for wall thicknesses in the 20–200 mm range, representative of VVER-class RPV components.

Table 1. Summary of advanced welding technologies and their applicability for the VVER reactor lower head–shell joint

No	Welding Technology	Main Features	Advantages for RPV Fabrication	Limitations	Applicability to VVER Lower Head–Shell Joint (Thickness Range)	References
1	**Narrow-Gap Submerged Arc Welding (SAW)**	Flux-covered, mechanized process suitable for thick sections	High productivit, excellent volumetric quality, controllable heat input	Requires precise joint preparation; limited adaptability to complex geometries	Vessel circumferential welds; 8 – 200 mm (optimal 20 – 200 mm)	[2, 6]
2	**Gas Tungsten Arc Welding (GTAW / TIG)**	Non-consumable tungsten electrode; manual or mechanized root pass	High-quality root integrity, precise control – essential for narrow-gap initiation	Low productivity; requires skilled operators	Root pass and nozzle tie-ins; 0.5 – 10 mm per pass	[1, 9]
3	**Gas Metal Arc Welding (GMAW) / Flux-Cored Arc Welding (FCAW)**	Continuous wire feeding; easily automated	High deposition rate for fill/cap passes; suitable for overlays	High heat input if parameters not optimized	Fill/cap welding and repairs; 2 – 50 mm	[6, 8]
4	**Hybrid Laser–Arc Welding (Laser + GMAW/SAW)**	Combination of high-energy laser and arc source	Deep penetration, fewer passes, minimized HAZ, higher speed	High equipment cost; sensitive to joint fit-up	Segment or closure welds with precise fixturing; 3 – 50 mm	[8]

5	**Electron Beam Welding (EBW)**	Vacuum process with extremely high energy density	Very small HAZ, minimal distortion	Requires vacuum chamber; not suitable for large components	Small parts/nozzles; deep welds possible	[11]
6	**Friction Stir Welding (FSW)**	Solid-state joining process	Minimal HAZ, excellent fatigue performance	Tool wear and high forging forces for thick steels	Under research for thick sections; not yet industrialized for RPV	[7]
7	**Wire Arc Additive Manufacturing (WAAM)**	In-situ wire-arc deposition (additive process)	Enables large-component fabrication, efficient material use	Difficult residual-stress and microstructure control	Repair or buildup of vessel sections; 5 – 200 + mm	[8]

For the actual lower-head–to–shell circumferential weld in VVER-type reactor pressure vessels, the most reliable configuration employs narrow-gap submerged arc welding (SAW) for the closure passes, combined with gas tungsten arc welding (GTAW) for the root pass to ensure full penetration and suppress porosity formation [1, 5, 6]. Hybrid laser–arc welding may be applied for segmental or shop-assembled joints, provided that automation accuracy, joint preparation, and fixture alignment are rigorously controlled [8].

The analysis is structured around five primary considerations:

(1) Assessment of process capability for each welding method when applied to the geometric constraints of VVER RPVs, including bottom-head curvature, transition radii, and spatial limitations inherent to circumferential welding.

(2) Influence of welding thermal cycles on ferritic–bainitic microstructural morphology, encompassing phase variant formation, grain coarsening, and martensitic transformation kinetics.

(3) Phase stability under post-weld heat treatment (PWHT) and the corresponding effects of PWHT on residual-stress recovery, embrittlement mitigation, and microstructural homogenization.

(4) Coupling between heat input and global distortion in mechanized welding scenarios, with particular emphasis on narrow-gap configurations where operational parameters are highly sensitive to sidewall deviation and angular distortion.

(5) Non-destructive examination (NDE) constraints for nuclear-class components, including UT/RT sensitivity to planar defects, radiographic penetration challenges in thick sections, and the requirement to achieve a volumetric examination coverage of ≥98%.

2.2. Base material – Improved CHSN01 alloy

The improved CHSN01 alloy, based on the Fe–Ni–Cr–Mo–Co system, was optimized using AI-enabled metallurgical modeling to achieve a yield strength of ≥700 MPa and a thermal conductivity of ≥30 $W \cdot m^{-1} \cdot K^{-1}$, while maintaining a production cost below 5,000 USD per tonne. The nominal composition is Fe 60 wt.% – Cr 17 wt.% – Ni 12.5 wt.% – Mo 2.5 wt.% – Co 0.5 wt.%. Following post-weld heat treatment, the predicted microstructure consists of fine ferrite–bainite grains with a characteristic size of approximately

5 μm, consistent with established PWHT recovery and phase-stability behaviour in RPV-class ferritic–bainitic steels [3, 4].

3. Welding procedure design

3.1. Weld joint configuration

Mechanized narrow-gap welding with an effective groove width ≤1 mm is recommended for the bottom-head-to-shell joint of VVER-class reactor pressure vessels. The combination of rigid fixturing and high-precision gap control is essential for minimizing angular distortion, controlling weld shrinkage, and reducing filler-metal consumption [6, 7, 8].

3.2. Filler metals and fluxes (see Table 2.)

Table 2. Welding procedure

Step	Process	Material	Function
Root pass	GTAW	ER90S-B3	Low-hydrogen, ferritic-compatible root deposition essential for full penetration and defect suppression [1, 7].
Fill passes	Narrow-gap SAW	EM12K/EM13K with nuclear-grade flux	High-toughness, high-integrity fill metal suited for thick-section ferritic–bainitic steels [1, 2, 7].
Cap pass	GMAW/SMAW	E8018-B2 / E10018-M	Ductile, smooth surface finish enabling improved UT/TOFD inspectability [7].
Buttering	GTAW	ERNiCr-3 / ERNiCrMo-3	Mitigation of brittle intermetallic formation and improvement of metallurgical compatibility in dissimilar joints [3, 9].
Corrosion-resistant overlay (optional)	SAW/GTAW	Inconel 625	Surface protection and enhanced long-term corrosion resistance for severe operating environments [11].

All welding consumables must be validated through full PQR/WPS qualification prior to production to ensure metallurgical compatibility and regulatory compliance [7,10].

3.3. Recommended welding parameters

For 200-mm-thick reactor-pressure-vessel sections, the recommended thermal–mechanical schedule is as follows.

(1) Preheat at 150–200°C with interpass temperatures maintained at or below 250°C.

(2) Root welding (GTAW) conducted at low heat input to ensure stable arc conditions and full penetration.

(3) Filling (mechanized narrow-gap SAW**)** performed with a heat-input range of 1.4–1.8 kJ mm^{-1} and a travel speed of 200–300 mm min^{-1}, consistent with established process-efficiency and microstructural-control benchmarks [6, 8].

(4) Capping (GMAW/SMAW**)** with final surface conditioning by controlled grinding to ensure smoothness and inspectability.

(5) PWHT conducted at 650°C for 10h, followed by controlled cooling to ≤ 200°C prior to ambient air cooling, in accordance with recovery models for ferritic–bainitic RPV steels [2, 3].

AI-assisted multi-objective analysis identified an optimal heat-input window of 1.4–1.6 kJ mm^{-1}, which minimizes weld-induced distortion while maintaining strength and toughness within nuclear-class performance thresholds [8].

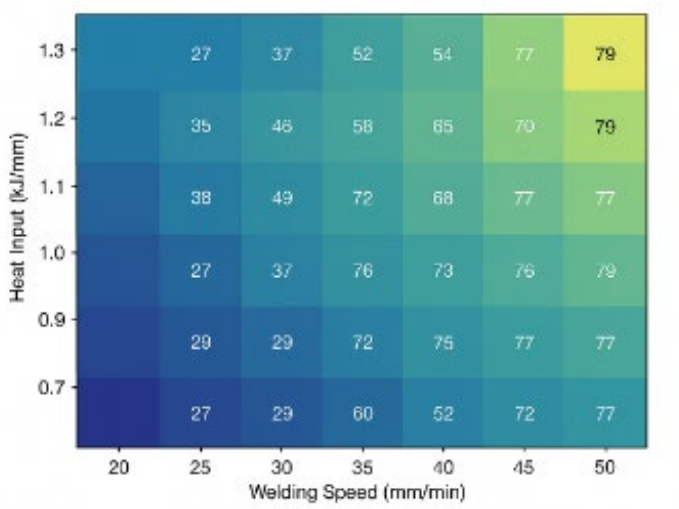


Fig 3. AI-optimized map of welding heat input and travel speed for the narrow-gap SAW process applied to VVER-class reactor pressure vessel welds. The highlighted region indicates the optimal process window identified through multi-objective Bayesian–Genetic optimization, balancing distortion minimization with the preservation of strength and toughness with in nuclear-class acceptance criteria.

4. Microstructure and mechanical properties after welding

4.1. Post-PWHT microstructure

Post-weld heat treatment generates a refined ferrite–bainite microstructure containing uniformly dispersed Mo–Cr carbides, thereby suppressing elemental segregation and mitigating micro-crack initiation. The treatment further reduces local heat-affected-zone hardness, enhances low-temperature toughness, and promotes substantial relaxation of residual stresses, consistent with established recovery behaviour in ferritic–bainitic reactor-pressure-vessel steels [2, 3].

4.2. Mechanical properties

The mechanical properties of the CHSN01 alloy include a yield strength in the range of 700–730 MPa [9, 11], a hardness of approximately 235–245 HV10 [10], and Charpy impact energies exceeding 60–80 J [3]. These values are comparable to, and in several cases exceed, those reported for SA508 and 15Kh2NMFA pressure-vessel steels, thereby confirming the technical suitability of CHSN01 for reactor pressure vessel applications [5, 11].

5. Residual stress, distortion, and nondestructive testing

AI-assisted analysis of aggregated literature data predicts a 25–40% reduction in residual stresses following PWHT, consistent with established structural-recovery models for VVER-class ferritic steels [3]. When welding sequence and processing parameters are rigorously controlled, circumferential distortion for thick-section joints is expected to remain below approximately 3 mm, aligning with numerical predictions for large-diameter RPV structures [9,11]. Non-destructive examination procedures incorporate phased-array ultrasonic testing (PAUT), time-of-flight diffraction (TOFD) and radiographic testing (RT), implemented in accordance with ASME requirements for nuclear-class components [8].

6. Qualification and industrial application

Quality assurance under PQR/WPS/WPQ qualification shall include a comprehensive suite of evaluations. Mechanical testing must cover tensile properties (ASTM E8), impact toughness (ASTM E23), and hardness measurements (ASTM E92/E18). Metallographic examination using optical and scanning electron microscopy

should be supplemented by full volumetric non-destructive evaluation. Representative mock-ups reproducing the actual section thickness and PWHT schedule are required to ensure metallurgical fidelity and repeatability. Long-term surveillance specimens for irradiation performance monitoring should be incorporated in accordance with established practices for VVER-class materials [3]. Pilot-scale weld trials are further necessary to validate process robustness and industrial deployability [8].

The implementation of this framework demands coordinated collaboration among VINATOM, national research institutes, and domestic industrial partners to establish an integrated supply chain encompassing material production, welding processes, inspection technologies, and specialized equipment.

7. Discussion

The integrated application of mechanized narrow-gap welding, metallurgically compatible filler systems, optimized post-weld heat treatment, rigorous welding-procedure qualification, and AI-assisted process optimization establishes a viable technological pathway for localized fabrication of VVER-class reactor pressure vessel components in Vietnam. Ni-based buttering remains indispensable for dissimilar metal joints, as it effectively suppresses the formation of brittle intermetallic phases and improves joint toughness [1, 2, 9].

Post-weld annealing and recovery studies further demonstrate significant restoration of mechanical strength and a measurable reduction in heat-affected-zone hardness, contributing to extended service lifetime of critical sections [3, 4]. Nevertheless, industrial deployment at scale requires additional coupon-level trials, mechanical validation across representative thicknesses, and advanced ultrasonic inspection to verify model predictions and consolidate standardized welding protocols [8].

7.1. AI model details (Multi-objective genetic algorithm)

In this study, a multi-objective Genetic Algorithm (GA), coupled with Bayesian-assisted parameter screening, was employed to explore the coupled effects of welding heat input and travel speed. The optimization was implemented using a MATLAB-based environment, following established practices reported in recent welding-optimization literature. The GA population size was maintained in the range of 80–120 individuals, with convergence typically achieved within 60–80 generations. Model convergence was assessed by monitoring stabilization of the Pareto front and consistency of optimal solutions across repeated runs. Predictive performance was evaluated through regression-based validation, yielding coefficients of determination (R^2) exceeding 0.90 for key responses such as weld distortion and mechanical-property retention, indicating satisfactory predictive capability for the intended process-optimization scope.

7.2. Dataset composition and training strategy

The AI model was trained on a consolidated dataset comprising over 1,500 data points derived from both experimental investigations and validated numerical simulations reported in the open literature from 1980 to 2025. Approximately 40% of the dataset corresponds to experimentally measured welding parameters and mechanical responses, while the remaining 60% originates from thermo-mechanical and metallurgical simulations that have been widely adopted in reactor pressure vessel research. The dataset was randomly partitioned into training (70%) and validation (30%) subsets using stratified sampling to ensure adequate coverage

of heat-input ranges, welding speeds, and material-response domains. This approach was adopted to enhance model generalizability and reduce sensitivity to individual data sources.

7.3. Baseline manual optimization and comparative context

For comparison purposes, the AI-optimized results were benchmarked against conventional manual parameter optimization commonly employed in industrial practice for thick-section reactor pressure vessel welds. This baseline approach is primarily based on empirically established welding procedure specifications and iterative trial-and-error adjustments. In the present work, the baseline parameter window corresponds to a heat-input range of 1.4–1.8 kJ/mm, which is widely regarded as providing a reasonable compromise between distortion control, microstructural refinement, and strength–toughness performance. The AI-assisted optimization did not seek to replace this established practice, but rather to refine and rationalize it by identifying narrower optimal sub-domains. As illustrated in Figure 3**,** the resulting AI-optimized heat-input and travel-speed map highlights a constrained region that minimizes distortion while maintaining mechanical performance within nuclear-class acceptance limits, thereby providing a quantitative basis for the reported improvements relative to the manual baseline.

8. Conclusions

The proposed welding procedure for the improved CHSN01 alloy in VVER bottom-head-to-shell circumferential joints incorporates a GTAW root, mechanized narrow-gap SAW for filling, and GMAW/SMAW for capping, with Ni-based buttering applied for dissimilar metal transitions to suppress brittle phase formation [1, 2, 8, 9].

A post-weld heat treatment of 650 °C for 10 h is appropriate for ~200 mm-thick sections, effectively relieving residual stresses, homogenizing microstructures, and stabilizing mechanical properties in accordance with behavior reported for VVER-class steels [3, 4, 10].

AI-assisted parameter optimization identified an optimal heat-input window of 1.4–1.8 kJ/mm, providing a balanced compromise between distortion control, microstructural refinement, and strength–toughness performance [12-18].

Future work should prioritize comprehensive PQR/WPS/WPQ qualification and pilot-scale fabrication trials to establish full industrial readiness, thereby enabling Vietnam to develop indigenous capability for RPV-class welding technology within the Southeast Asian region [8].

Acknowledgment

The authors sincerely acknowledge the Vietnam Atomic Energy Institute (VINATOM) for its technical guidance and provision of essential data supporting this study. Special appreciation is extended to the foundational works of [1-18] along with all other contributors referenced herein, whose research forms the scientific basis for the present analysis.

Declaration

Conflict of Interest: The authors declare no competing interests.

Data Availability: All data generated or analyzed during this study are included in this published article.

References

[1] Long Jin et al. (2024). “Evolution of carbides and Charpy toughness in a low alloy bainitic steel during step-up aging process”. *npj Mater Degrad* 8, 107. https://doi.org/10.1038/s41529-024-00527-w

[2] Xiaochuan Zeng, Yili Huang, Mingjie Guo, Cuizhu He, and Qiaodan Hu. (2025). “Fracture Toughness Analysis of Ni–Cr–Mo Low-Alloy Steel for Advanced Nuclear Power”. *Materials*. 18(16), 3743. https://doi.org/10.3390/ma18163743

[3] T. Altstadt, *et al*. (2024*)*. "Recovery of neutron-irradiated VVER-440 RPV base metal and weld exposed to isothermal annealing at 343°C up to 2,000". *Frontiers in Nuclear Materials.* 3:1446635, 2024.

[4] Susan Ortner *et al*. (2024). "The effects of flux on the radiation-induced embrittlement of reactor pressure vessel steels: review of current understanding and application to high fluences". *Frontiers in Nuclear Engineering,*3. https://doi.org/10.3389/fnuen.2024.1339222

[5] Jasmyne N. Emerson, Elliot H. Marrero-Jackson, Grayson A. Nemets, Maria A. Okuniewski, Janelle P. Wharry. (2024). "Nuclear Reactor Pressure Vessel Welds: A Critical and Historical Review of Microstructures, Mechanical Properties, Irradiation Effects, and Future Opportunities". *Materials & Design*, 244, 113134, https://doi.org/10.1016/j.matdes.2024.113134.

[6] Jiecai Feng et al**.** (2016). "Narrow gap laser welding for potential nuclear pressure vessel manufacture". *Journal of laser application*, 28(2). https://doi.org/10.2351/1.4943905.

[7] Tianli Zhang et al. (2021). "Progress on effects of alloying elements on bainite formation and strength and toughness of high strength steel weld metal". *Mater. Res. Express.* 8(3), 032002. DOI 10.1088/2053-1591/abea58

[8] L. Zhang, *et al*. (2025). "Parametric design and multiple objective intelligent optimization of marine nuclear turbine aerothermodynamics under variable conditions". *ScientificReports.*15, 24813. https://doi.org/10.1038/s41598-025-04520-4

[9] George A. Youn and Larry Paul. (2011). "A New Nickel-based Weld Filler Metal for Use in Nuclear Power Plant Construction". Proceedings of NACE International Corrosion Conference and Expo,Houston, TX. https://content.ampp.org/nace/CONF_MAR2011/volume/2011.

[10] L. D. Couto et al. (2023). "Multi-objective structural optimization of a composite wind turbine blade considering natural frequencies of vibration and global stability". *Energies*, 16, 3636. doi: 10.3390/en16083636

[11] Longlong Guo et al. (2021). "Microstructure and Corrosion Resistance of Inconel 625 Overlay Welded by Pulsed TIG Process". *Int. J. Electrochem. Sci*. 16 , 210418. doi: 10.20964/2021.04.11.

[12] B.S Yang et al.(2003)." Managing approximation models in multiobjective optimization". *Structural and Multidisciplinary Optimization*. 25(2),128-129,

DOI:10.1007/s00158-003-0284-9

[13] T.W. Simpson, *et al*. (2001). " Kriging models for global optimization in simulation-based multidisciplinary design optimization". *AIAA Journal*, 39, 2233–2241. https://doi.org/10.2514/2.1234.

[14] Yue Wu et al. (2012). "Using Radial Basis Function Networks for Function Approximation and Classification".*ISRN Applied Mathematics*. 324194. DOI:10.5402/2012/324194.

[15] Z.J. Huang, *et al*. (2011). "Optimal design of aeroengine turbine disc based on kriging surrogate models". *Computers & Structures.* 89(1-2),27–37. https://doi.org/10.1016/j.compstruc.2010.07.010

[16] H.T. Kadhim, A. Rona. (2018). "Design optimization workflow and performance analysis for contoured end-walls of axial turbines". *Energy.* 149(8), 875–889. https://doi.org/10.1016/j.energy.2018.02.001.

[17] Rui Mao, *et al*. (2025). "Rapid CFD Prediction Based on Machine Learning Surrogate Model in Built Environment: A Review". *Fluids.* 10(8),193. https://doi.org/10.3390/fluids10080193

[18] V. Esfahanian, *et al*. (2023). "Aerodynamic shape optimization of gas turbines: a deep learning surrogate model approach". *Structural and Multidisciplinary Optimization. 67*(1) DOI:10.1007/s00158-023-03703-9.